Molecular BioSystems

Accepted Manuscript

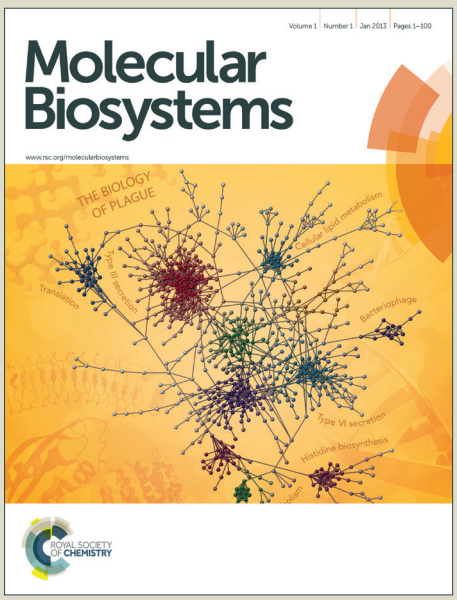

ROYAL SOCIETY OF CHEMISTRY

www.rsc.org/molecularbiosystems

A putative role of the Sup35p C-terminal domain in the cytoskeleton organization during yeast mitosis

Insung Na,[1] Krishna D. Reddy,[1] Leonid Breydo,[1] Bin Xue,[2] and Vladimir N. Uversky[1,3,4*]

[1]Department of Molecular Medicine, Morsani College of Medicine, University of South Florida, Tampa, Florida 33612, USA

[2]Department of Cell Biology, Microbiology, and Molecular Biology, College of Arts and Science, University of South Florida, Tampa, Florida 33612, USA

[3]USF Health Byrd Alzheimer's Research Institute, Morsani College of Medicine, University of South Florida, Tampa, Florida 33612, USA

[4]Institute for Biological Instrumentation, Russian Academy of Sciences, 142290 Pushchino, Moscow Region, Russia

Abstract

Sup35 protein (Sup35p), or eukaryotic peptide chain release factor GTP binding subunit (eRF3), is a well-known yeast prion responsible for the characteristic [*PSI*$^{+}$] trait. N- and M-domains of this protein have been foci of intensive research due to their importance for the prion formation. Sup35p C-terminal domain (Sup35pC) is essential for translation termination and cell viability. Deletion of Sup35pC was shown to lead to the malformation of cells during mitosis. In this study we confirm that Sup35pC domain possesses high sequence and structural similarity to the eukaryotic translation elongation factor 1-α (eEF1A) from yeast and show that its sequence is conserved across different species including human. Because cell malformation during mitosis could be due to the deregulation of cytoskeleton formation, and since a Sup35 paralog eEF1A is known to act as an actin modulating protein, we focused on establishing of the relationships between the Sup35pC and modulation of the cytoskeleton formation. We found 104 co-partners between Sup35pC and EF1A of *S. cerevisiae*, and 18 partners of human ERF3A. Based on the analysis of known and modeled structures of some effectors and partners we found possible protein-protein interactions. Based on our study, we propose that Sup35pC may serve as actin modulator during mitosis.

Key words: yeast prion; Sup35p; actin; eukaryotic translation elongation factor; heat shock protein

Introduction

Saccharomyces cerevisiae peptide chain release factor GTP binding subunit 3 (eRF3) is encoded by the *SUP35* gene and known as the Sup35 protein (Sup35p). Sup35p is a prion-forming functional protein whose primary function is translation termination activity during protein biosynthesis,[1-3] where it cooperates with the eukaryotic peptide chain release factor GTP binding subunit 1 (eRF1) when stop codon is recognized.[4, 5] However, it also forms one of the yeast prion phenotypes, [*PSI*$^+$], which is non-mendelian in its passage to progeny cells.[6-9] *S. cerevisiae* Sup35p is a 685 amino acid long protein consisting of the N-terminal prion-forming domain (PrD or N-domain, residues 1-123), highly charged middle domain (M-domain, residues 124-253), and the C-terminal domain (C-domain, residues 254-685).

The capability of Sup35p to form and maintain fungus prion ([*PSI*$^+$] phenotype) is encoded in the structural characteristics of the prion forming, Q/N-rich N-terminal domain of Sup35p.[10-15] The Sup35p-PrD is characterized by unusual amino acid composition containing 43% glutamine/asparagine residues.[16] The extreme N-terminal region (amino acids 8–33) is particularly rich in glutamine/asparagine residues, and this is followed by the region composed of five complete copies (R1–R5) and one partial copy (R6) of an imperfect oligopeptide repeat with the consensus sequence PQGGYQQ-YN. The Sup35p M-domain plays a role in the prion formation by serving as an aggregation controller,[17, 18] whereas C-domain, being inessential for aggregation,[19, 20] is responsible for the translation-termination activity of this protein.[21]

Hsp104 chaperone plays an important role in propagation of Sup35 prion by fragmenting Sup35 fibrils to create propagation seeds (propagons).[1, 12, 22, 23] It has been also shown that in addition to Hsp104, the [*PSI*$^+$] forming area in yeast cells contains several other heat shock proteins, such as Hsp70 proteins (Ssa1/2 and Sse1) and the Hsp40 protein Sis1.[24] Recent *in silico* studies implementing molecular dynamics simulations suggested that ATP hydrolysis-based allostery of Hsp70 is important for prion propagation.[25, 26]

Among other functions, heat shock proteins are involved in the formation and maintenance of the cytoskeleton.[27] Here, an oligomeric complex known as chaperonin containing TCP-1 (CCT, also known as TRiC for the TCP-1 ring complex) serves as the eukaryotic cytoplasmic chaperonin which directs folding of cytoskeletal proteins such as α/β/γ-tubulin, actin, and centractin.[27, 28] From the set of heat shock proteins related to prion formation and propagation in yeast,[24] we focused on Hsp70 due to its potential roles in both prion seeding and actin maintenance.[29-31] It has been shown that Hsp70 and Hsp90 might act in a concerted manner as the CCT upstream factors by transferring the substrate to CCT,[29] where the proper protein folding of target proteins such as actin and tubulin is fine-tuned.[32, 33] Furthermore, it was shown that CCT interacts with F-actin and influences the cell shape and cytoskeleton assembly.[34] These observations suggest that the Hsp70 plays a role in the control of actin folding.

Among its other functions, eukaryotic translation elongation factor 1-α (eEF1A) is responsible for the cytoskeleton organization through its direct and indirect modulation of actin activity.[35] Direct interaction between eEF1A and actin has been described in several organisms such as *Zea mays*,[36] *Tetrahymena pyriformis*,[37, 38] and *S. cerevisiae*.[39] Also, it has been shown that there is an indirect effect of eEF1A on modulation of actin function.[40] Besides, a direct interaction between the eukaryotic elongation factor 1 (eEF1) and Ssa1, a yeast Hsp70 analog (also known as heat shock protein YG100), has been reported.[41] The spatial structure of eEF1A is very similar to that of Sup35pC of *Schizosaccharomyces pombe*[42] suggesting that Sup35pC may also directly or indirectly affect the actin function.

The purpose of this study was to examine the possibility that Sup35pC possesses a role in the cytoskeleton organization via actin modulation. To establish the degree of conservation of the *S. cerevisiae* Sup35p, we performed BLAST analysis of this protein against proteomes of ten eukaryotic species ranging from yeast to human. Among proteins with high sequence similarity to Sup35p, a human protein, eukaryotic peptide chain release factor GTP binding subunit (ERF3A) encoded by the *GSPT1* gene, was chosen. Because ERF3A is indirectly linked to actin

modulation via the mTORc2 pathway,[43-47] through the interaction with phosphatidylinositol 3-kinase regulatory subunit alpha (PIK3R1) and protein kinase B (AKT), PIK3R1 was chosen as a potential target for subsequent analysis. We assigned Sup35pC, EF1A of *S. cerevisiae,* and eRF3A of human as effectors. We assumed that actin and Hsp70 proteins, such as Ssa1 of *S. cerevisiae,* and PIK3R1 of human can serve as partners of the mentioned effectors.

In our analysis, we looked for sequence similarity, conserved family, motifs, and protein intrinsic disorder-based binding sites, molecular recognition features (MoRFs).[48] We found 104 co-partners between Sup35pC and EF1A of *S. cerevisiae,* and 18 partners of human ERF3A. To verify the possible interactions between effectors and partners, we obtained PDB structures for some proteins and modeled structures for other proteins which next were used to find possible protein-protein interactions. These analyses resulted in finding possible interactions between effectors and partners. Based on our study, we propose that Sup35pC may serve as actin modulator during mitosis.

Materials and Methods

Establishing sequence similarity between EF1A and Sup35pC of *S. cerevisiae*

To show sequence similarity between EF1A and Sup35pC of *S. cerevisiae,* we performed sequence alignment between two proteins through CLUSTAL Omega 1.2.0 on the database, UniProt (http://www.uniprot.org).[49] The UniProt identifiers for these proteins are P02994, and P05453, respectively. Since the Sup35pC is a C-terminal domain of eRF3, we obtained the corresponding sequence spanning residues 254-685 of the P05453 and defined it as Sup35pC as it done throughout literature.[1]

Verification of the Sup35pC conservation among different eukaryotic species

To find evolutionary conserved patterns of the Sup35pC sequence, we performed the protein sequence oriented BLAST analysis using the BLASTP algorithm (http://blast.ncbi.nlm.nih.gov),

where ten reference organisms, *Saccharomyces cerevisiae* (taxid:4932), *Caenorhabditis elegans* (taxid:6239), *Drosophila melanogaster* (taxid:7227), *Ciona intestinalis* (taxid:7719), *Oryzias latipes* (taxid:8090), *Danio rerio* (taxid:7955), *Xenopus tropicalis* (taxid:8364), *Gallus gallus* (taxid:9031), *Mus musculus* (taxid:10090), and *Homo sapiens* (taxid:9606), were chosen from the NCBI Reference Sequence Database (RefSeq, http://www.ncbi.nlm.nih.gov/refseq/). In this analysis, Sup35pC sequence was used as a query sequence and most similar proteins of each organism were chosen for subsequent studies. Next, sequence alignment was performed using the CLUSTAL Omega 1.2.0 algorithm,[49] for which sequences of identified proteins were found in the UniProt database (see Table 1 for the lists of proteins and their corresponding IDs). To specifically focus on Sup35pC domain, an additional sequence alignment was performed using the CLUSTAL Omega 1.2.0 after sequence adjustment by Python, version 3.3.

Structural alignment using PyMOL 1.3

For structural alignments, the PyMOL program 'Align' and 'CEAlign' functions were used. In the case of the structural alignment of effectors, the 'Align' function was used due to their high sequence similarities. However, in case of the structural alignment of partners, which do not possess meaningful sequence similarity, the 'CEAlign' function was used. In detail, during the structural analysis of the effectors, model structures of Sup35p (amino acids 243-685), and ERF3A (amino acids 72-495) were obtained from the SWISS_MODEL Repository (http://swissmodel.expasy.org), which were based on the eEF1alpha-like region of eRF3 from *S. pombe* (PDB ID: 1R5B, http://www.rcsb.org).[42, 50, 51] Sequence similarities between the Sup35p (amino acids 243-685) and ERF3A (amino acids 72-495) and the eEF1alpha-like region of Sup35p from *S. pombe* were 58.3%, and 47.7%, respectively. Structure of the EF1A protein was obtained from PDB (PDB ID: 1F60).[52] For domain structural similarity analysis among effectors, structures were fragmented according to the sequence homology among effectors (Figure 1) and domain information on EF1A.[39, 42]

For the structural alignment of partners, structures of actin (residues 1-375, PDB ID: 1YAG)[53] and fragments comprising residues 3-85, 115-309, and 614-724 of PIK3R1 (PDB IDs: 1PHT, 1PBW, and 1BFI, respectively)[54-56] were used. Although 1BFI is a portion of the *Bos taurus* protein, we used this structure, since sequence of this fragment of bovine PIK3R1 is 100% identical to the corresponding segment of human PIK3R1. Model structures of Ssa1 (4-544, model based on 3C7N), and some parts of PIK3R1 (residues 324-433 and 431-600 modeled based on structures 2IUG and 2V1Y, respectively) were retrieved from the SWISS_MODEL Repository.[50, 51] Structures of Ssa1 and actin were fragmented according to the earlier published alignment results.[57] The resulting fragmented structures were superimposed using 'CEAlign' function of PyMOL.

After sequence alignment and finding conserved motif and MoRF (Figure 3B), we focused on the MoRF regions. At this stage, we performed 'Align' and 'CEAlign' functions of PyMOL were used to search for structural similarity between actin fragment (residues 7-98) and PIK3R1 fragment (residues 3-85). The reason of using 'Align' function is noticeable sequence similarity of these two fragments.

Search for the *S. cerevisiae* partners of Sup35pC and EF1A and the *H. sapiens* partners of ERF3A

To find the *S. cerevisiae* partners of Sup35p and EF1A and the human ERF3A partners the PSICQUIC database was used (http://www.ebi.ac.uk/Tools/webservices/psicquic/view/).[58] Among the yeast partners of Sup35p and EF1A, 104 interactors were selected. 104 interactors of two yeast proteins represent an intersection of these proteins' partner sets. The analogous analysis produced 18 partners for the human ERF3A. At this step, all partners of human ERF3A were chosen. To obtain sequences of all these proteins in FASTA format, proteome information on *S. cerevisiae*, and *H. sapiens* was downloaded from UniProt. Sequence similarity scores for the 104 partners of *S. cerevisiae* Sup35pC and EF1A and the 18 partners of *H. sapiens* ERF3A

were obtained by a computational tool designed using Python (version 3.3) and its modules, such as BioPython (version 1.62b) and NumPy (version 1.7).

To measure ranks among similarity scores of 104 partners of yeast Sup35p and EF1A with certain partner of human ERF3A, codes were designed to perform 1872 (104 × 18) sequence alignments. To this end, BLOSUM62 based pairwise2 module in BioPython were used at each alignment.[59] Among the resulting hits, functionally related partners (such as *S. cerevisiae* Ssa1 and actin, and *H. sapiens* PIK3R1) were found as described in the Introduction section.

Search for the conserved domains, motifs, and molecular recognition features (MoRFs), and intrinsic disorder analysis

To find conserved domains, the Pfam database (http://pfam.sanger.ac.uk/) was used.[60] To find possible PfamB hits, the corresponding sequences in FASTA format were directly put to the submission panel with default settings except for selection for PfamB. The search for functional motifs was performed using the ELM database (http://elm.eu.org/).[61] During this analysis, the already assigned UniProt IDs the proteins were used for submission without modification of the default settings (Table 2). MoRFs were found using the MoRFpred algorithm (http://biomine-ws.ece.ualberta.ca/MoRFpred/index.html).[48] The amino acid sequences which showed probability values greater than 0.5 were chosen among the retrieved results.

To visualize the results, the sequence alignments by CLUSTAL Omega 1.2.0 were performed separately among the effectors and partners. Continuously, the common MoRFs containing ELMs were highlighted directly within the corresponding text files (Figure 3). To get information on the conserved amino acids, MoRF, and motif containing regions, the motif names were not discriminated.

To specifically focus on the disordered region in the specific parts of query proteins, such as the 1-111 regions of actin and Ssa1, and the 614 – 724 region of PIK3R1, the PONDR-FIT algorithm was used.[62]

Interaction prediction

Based on the results of previous analyses,[57] the possible interactivities of the analyzed proteins were predicted using the iLoops algorithm.[63] The whole sequences of Sup35pC, EF1A, ERF3A, and PIK3R1, and partial sequences of actin (8-349), and Ssa1 (7-376) were used in this analysis (Table 2), during which, four pairs, Sup35pC *vs*. Ssa1 (7-376), EF1A *vs*. actin (8-349), ERF3A *vs*. PIK3R1, and Sup35pC *vs*. actin (8-349) were matched.

Results

Amino acid sequence and structural similarity of the *S. cerevisiae* Sup35pC and EF1A

The existence of the overall structural similarity between the C-terminal fragment of Sup35p (Sup35pC) and *S. cerevisiae* EF1A has been already reported.[42, 64] However, despite the fact that both proteins possess complex multidomain structure, the similarity at the domain level was not studied as of yet. Since domains are important functional entities of many proteins, we focused on the analysis of the domain-wise structural similarities.

Figure 1A represents the results of the sequence alignment of the Sup35pC and EF1A and shows that proteins possess significant similarity at the sequence level, being 35.1% identical. Figure 1B represents the output of the structural alignment of the full-length proteins and shows that although proteins possess noticeable structural similarity, due to the noticeable relative disposition of domains and the pronounced dislocation of α-helices in the domain 1, the overall root mean squared deviation (RMSD) value appeared high, 17.6 Å. Finally, Figure 1C shows that the structural alignment was dramatically improved when three protein domains were analyzed individually. Here, the retrieved RMSD values were meaningfully decreased in comparison with the RMSD of the aligned full-length chains. The RMSD of the domain 1 alignment (2.02 Å) was noticeably higher than RMSDs for domains 2 and 3 (0.864 Å and 0.997

Å, respectively). Figure 1C also shows that the major reason for the domain 1 structural variability is caused by the dislocation of several α-helices.

Based on the existence of significant structural similarity between the Sup35pC and EF1A and the fact that EF1A is involved in the cytoskeleton organization, we hypothesized that one of the Sup35pC functions could be related to actin modulation. In fact, this hypothesis is supported by the results of the experimental analysis of the effects of the *SUP35* gene repression on the yeast morphology.[65] Here, the repression of the *SUP35* gene was shown to result in the accumulation of cells of increased size with large buds caused by the disappearance of actin cytoskeletal structures and accompanied by the impairment of the mitotic spindle structure and defects in nuclei division and segregation in mitosis.[65] Although the direct involvement of Sup35pC in modulation of actin cytoskeleton is an attractive hypothesis, it is also possible that the repression of the *SUP35* gene has more general effects on translation.

High conservation of Sup35pC-like sequences among ten eukaryotic organisms

The existence of some sequence similarity between the *S. cerevisiae* Sup35pC and the eRF3 proteins of other organisms is has been established.[2] To evaluate the conservation of eRF3 proteins among ten different eukaryotic organisms, the BLASTP algorithm of the BLAST package was applied to the NCBI RefSeq database and for each organism, the most conserved sequence was chosen. Then, the amino acid sequences of these ten proteins were aligned using the CLUSTAL Omega Version 1.2.0 algorithm (see Table 1).

The analysis of the full-length sequences shows that the sequence identity among ten proteins was 22.1%. When focused exclusively on the Sup35pC, the identity increased to 36.7% (Table 3). This analysis showed that among 10 proteins there was only one identical position outside of the Sup35pC region, and the number of similar positions outside the Sup35pC region was very low. Therefore, this analysis revealed that most of the Sup35pC amino acids are highly conserved among ten eukaryotic organisms, whereas N- and M-domains are not meaningfully

conserved, despite the fact that most of the analyzed proteins are considered to have eRF3 activity.

Sequence similarities among the partners of the yeast Sup35p and EF1A and human ERF3A

At the next stage, we looked for the partners of the effectors (i.e., proteins of interest, yeast Sup35p and EF1A, and human ERF3A) as described in the Materials and Methods section. This search revealed 104 partners of two yeast proteins (Sup35p and EF1A), and 18 partners of a human protein ERF3A (Table 4). This analysis was based on the assumption that the Sup35pC partners are among the identified Sup35p partners. This assumption was necessary due to the lack of specific data on the Sup35pC binding partners. Special attention was paid to the partners potentially related to the modulation of the cytoskeletal structure, such as actin and Ssa1 from *S. cerevisiae*, and *H. sapiens* PIK3R1 (see Introduction section).

The amino acid sequences of the 104 partners of two yeast effectors (Sup35p and EF1A) were compared with the sequences of the 18 partners of a human effector protein ERF3A. To measure ranks among similarity scores of 104 partners of yeast Sup35p and EF1A with a certain partner of human ERF3A, 1872 (104 × 18) sequence alignments were performed, and 18 human proteins were roughly ranked by their similarity scores. This analysis revealed that the partner of interest, human PIK3R1 (UniProt ID: P27986), is ranked 6th among 18 human proteins (Table 5).

Similar analysis of the sequence similarities of the 104 partners of two yeast effectors, Sup35p and EF1A, revealed that the partners of interest, actin (UniProt ID: P60010) and Ssa1 (UniProt ID: P10591) are ranked 70th (score 1021) and 34th (score 1340), respectively (see Table 6). Finally, Table 7 represents the results of the sequence alignments by CLUSTAL Omega, Version 1.2.0 and shows that pair-wise identities were 8.7% and 13.2% for the pairs of PIK3R1-actin and PIK3R1-Ssa1, respectively.

Structural similarities among the partners of interest

At the next stage, we analyzed the structural similarity of the three partners of interest: actin, Ssa1, and PIK3R1. Since the overall structural similarity between actin and Ssa1 is known (these two proteins belong to a superfamily defined by a fold consisting of two domains with the topology β-β-β-α-β-α-β-α),[57] we focused on the structurally conserved regions of those two proteins, which are residues 8-349 in actin, and residues 7-376 in Ssa1. The PIK3R1 regions for structural analysis were selected as described in the Materials and Methods section.

Figure 2A represents the results of structural alignment of actin (residues 8-349) and Ssa1 (residues 7-376) and shows that structures of these two proteins are rather similar, being characterized by the RMSD of 5.04 Å. Since the known structure of Ssa1 represents the result of homology modeling, the experimentally determined structure of actin was used for the structural alignment of five different fragments of PIK3R1, residues 3-85, 115-309, 324-433, 431-600, and 614-724. Figures 2B-E represent the results of structural alignment of actin with four PIK3R1 fragments and shows that there is noticeable structural similarity between actin and PIK3R1 residues 3-85 (RMSD of 6.49 Å), 115-309 (RMSD of 8.61 Å), 324-433 (RMSD of 7.46 Å), and 614-724 (RMSD of 7.12 Å). Figure 2F shows that the 431-600 fragment of PIK3R1 lacks any structural similarity with actin.

Functional analysis of effectors and partners: Conserved domains, MoRFs, functional motifs, and disorder predictions

To find functional information, proteins of interest (effectors and their specific partners) were analyzed using Pfam, ELM, and MoRFpred resources as described in Materials and Methods section. Several conserved functional domains, such as GTP_EFTU, GTP_EFTU_D2, and GTP_EFTU_D3 were found in effectors. Here, GTP_EFTU and GTP_EFTU_D2 are the members of the P-loop containing nucleoside triphospate hydrolase superfamily (Table 8).

Similar Pfam-centric analysis of partners revealed that although the actin and Ssa1 domains belong to the different families, these two families are the members of one superfamily, actin-like ATPase as described at previous research (Table 8). This finding is in agreement with the results of earlier research.[57] However, PIK3R1 did not show meaningful functional domain homology with other partners.

Pfam provides reliable information on conserved functional domains in proteins. The identification of domain, which are defined as a conserved part of a given protein sequence and structure that can evolve, function, and exist independently of the rest of the protein chain, can provide insights into their function. However, besides functional domains which correspond to a rather sizable segment of an amino acid sequence, typically ranging from ~40 to ~700 residues,[66] many proteins contain short functional motifs and intrinsic disorder-based potential interaction sites, known as molecular recognition features, MoRFs. To find such conserved functional motifs and MoRF, proteins of interest were analyzed using ELM and MoRFpred engines, as described in the Materials and Methods section. The results of the MoRFpred analysis are shown in Table 9, whereas Table 10 represents the results of the ELM analysis.

When the results of these two analyses were superimposed with the results of the sequence alignments (see Figure 3), it became clear that effectors contain multiple conserved functional motifs and MoRFs and even one region that corresponded to the completely overlapped MoRFs and a unique functional motif, LIG_FHA_2 (Figure 3A, sequences located with the red box). Similar analysis of partners is shown in Figure 3B that illustrates that these proteins also possess one MoRF region that contains functional motif MOD_N-GLC_1 in actin and TRG_ENDOCYTIC_2 motif in Ssa1 and PIK3R1 (see Figure 3B, sequences located with the red box).

Among regions showing structural homology, we focused on the MoRF containing site of actin, residues 11-15 (Figure 2B, fourth structure alignment). Figure 4A shows that in the aligned structures, PIK3R1 fragment (residues 650-657, green) and actin fragment (residues 11-

15, red) possess similar patterns, namely β-loop-β motifs. Based on the above analysis (Figure 3B), we performed additional structural alignment between another PIK3R1 fragment (residues 3-85) and matched actin fragment (residues 7-98). However, there was no meaningful structural similarity between these fragments (data not shown).

Intrinsic disorder in actin, Ssa1, and PIK3R1

Figure 5 represents the results of intrinsic disorder propensity analysis of actin (Figure 5A), Ssa1 (Figure 5B), and PIK3R1 (Figure 5C). Due to the high sequence and structure heterogeneity of intrinsically disordered proteins,[67] the set of currently available disorder predictors is very large.[68] Therefore, the disorder probabilities in these three proteins of interest were evaluated by several algorithms, such as PONDR® VLXT,[69] PONDR® VL3,[70] and PONDR-FIT.[62] The choice of these predictors was determined by the peculiarities of their performance. In fact, although PONDR® VLXT is not the most accurate disorder predictor, it is exclusively sensitive to the peculiarities of the local compositional profile,[69] which makes it a suitable tool for finding potential disorder-based binding sites. These sites are located within long disordered regions and are typically defined as segments with the increased propensity to order that are flanked by the disordered regions. Many of these segments are recognized as Molecular Recognition Features (MoRFs) and are found to be very important for molecular recognition, signaling, and regulation.[71, 72] PONDR® VL3 is typically used for the accurate characterization of long disordered regions,[70, 73] whereas the meta-predictor nature of PONDR-FIT makes it one of the most accurate general predictors of intrinsic disorder in proteins.[62] Figure 5 clearly shows that all three proteins belong to the category of hybrid proteins possessing both ordered and intrinsically disordered regions.[74]

Assignment of actin to the category of hybrid proteins is not a trivial statement since this globular protein is known to possess 3D-structure (see below). Curiously, the available information on the structure of this protein is derived from its complexes with various actin

binding proteins (ABPs), such as DNase I (PDB ID: 1ATN),[75] a *Vibrio parahaemolyticus* effector protein VopL (PDB ID: 4M63),[76] chimera of gelsolin domain 1 and C-terminal domain of thymosin β-4 (PDB ID: 1T44),[77] and many other proteins. This is because of the strong intrinsic propensity of G-actin (globular form) to polymerize to fibrillar form (F-actin). Although this polymerization prevents G-actin from the crystal formation, it can be prevented via actin binding to some ABPs, and therefore it can be crystallized in the presence of these ABPs. In addition to the G- and F-forms, actin can be easily transformed into inactivated state, I-actin, in which the protein molecule loses its capability to polymerize. The transition to the I-actin can be initiated by the removal of calcium ion by the EDTA or EGTA treatment, removal of nucleotides (ATP or ADP), heat denaturation, exposure to moderate urea or GdnHCl concentrations, dialysis with 8 M urea or 6 M GdnHCl, or spontaneously during storage.[78-85] This inactivated actin is characterized by the intrinsic fluorescence spectrum with maximum at wavelength intermediate between the wavelengths of the native and completely unfolded protein,[82] combined with rather rigid microenvironment of tryptophan residues,[86] a considerable increase of the fluorescence anisotropy value reflecting a considerable decrease in the internal mobility of the tryptophan residues in the inactivated actin,[85] and a noticeable distortion of the secondary structure.[86] Recently, based on the detailed consideration of these and numerous other facts such as inability of actin to maintain folded native state without being involved in interaction either with small molecules (Ca^{2+}, ATP, ADP) of other proteins, its ability to interact with an enormous number of partners[87] and possesses numerous posttranslational modification sites, it has been concluded that this protein fits into the category of intrinsically disordered proteins.[88]

Figure 5D shows that although the overall disorder profiles of actin, Ssa1, and PIK3R1, are generally rather different, these proteins possess some local similarity between their N-terminal domains. This conclusion is further illustrated by Figure 5E which represents the overlapped

disorder profiles for the first 250 residues of these three proteins and shows that there is a noticeable similarity between the major disorder features.

Intrinsic disorder in Sup35p, EF1A, and ERF3A

Figure 6 represents results of the evaluation of intrinsic disorder propensity in Sup35p (Figure 6A), EF1A (Figure 6B), and ERF3A (Figure 6C) by three computational tools described above, PONDR® VLXT, PONDR® VL3, and PONDR-FIT. Figure 6 shows that the effector proteins analyzed in this study also belong to the category of hybrid proteins possessing both ordered and intrinsically disordered regions.[74] It is also evident that the N-terminal tail of the yeast Sup35p is highly disordered, whereas the disorder profile for the C-terminal region of this protein is rather similar to disorder profiles of EF1A and ERF3A (see Figure 6D). Therefore, results of disorder analysis provide further support to the conclusion on the similarity between the effector proteins, Sup35pC, EF1A, and ERF3A.

Prediction of protein-protein interactions between effectors and partners using the iLoops algorithm

To evaluate the probability that effectors and partners are involved in physical interactions, the iLoops Server (http://sbi.imim.es/iLoopsServer/) was used.[63] This server determines where a pair of proteins is involved in interactions based on the information on known protein interactions, putative non-interacting proteins, and various protein features, such as loops (as defined by ArchDB, http://sbi.imim.es/archdb/) and/or domains (as defined by SCOP, http://scop.mrc-lmb.cam.ac.uk/scop/).[63] Table 11 represents the results of this analysis and shows that there are four interacting pairs: Sup35pC-Ssa1 (residues 7-376), Sup35pC-actin (residues 8-349), EF1A-actin (residues 8-349), and ERF3A-PIK3R1 (see Supplementary Table 1). Therefore, these data suggest that effectors are likely to interact with expected partners.

Discussion

The purpose of this study was to evaluate the likelihood that Sup35p is involved in direct or indirect interaction with actin that ultimately can be related to new functional roles of Sup35p in the cytoskeleton organization. This hypothesis is based on two important observations made in previous studies. More discussion of these observations is provided below. Through sequence alignments and domain-based structural alignments of Sup35pC and EF1A we could infer the possibility of interaction between Sup35pC and actin in yeast. Both our results and earlier experimental data show that EF1A is one of the members of actin interactome. Sup35pC has previously been shown to be a paralog of EF1A[35, 42] and our sequence and structural alignment results show excellent alignment between the C-terminal domain of Sup35 and EF1a. Also, important morphological information is available on the malformation of yeast cells when Sup35pC is depleted.[65] Here, besides the rather obvious consequences of the shortage of the transcription terminator Sup35p, such as a reduction in the levels of the other release factor (Sup45p) and a substantial increase of nonsense codon readthrough, noticeable morphological effects were reported. For example, repression of the *SUP35* gene caused accumulation of cells of increased size with large buds accompanied by the disappearance of actin cytoskeletal structures, impairment of the mitotic spindle structure, and defects in nuclei division and segregation in mitosis.[65]

The sequence similarity analysis revealed that Sup35pC is highly conserved among ten eukaryotic organisms, ranging from yeast to human. Furthermore, of 160 conserved amino acids of these ten proteins, 159 residues were found within their Sup35pC regions. These results suggest that the biological functions of Sup35pC could be conserved from yeast to human too. One of the known functions of this C-terminal domain, which is known to be essential for the yeast growth, is its translation termination activity.[7, 10, 21, 89, 90] Despite some reports to the contrary,[91, 92] Sup35pC does not appear to be involved in [PSI^+] prion formation.[19, 20] The largely disordered NM region controlling prion formation in yeast is not evolutionary conserved,

since only one of the 160 identical amino acids found in ten eukaryotic eRF3 proteins appeared within this domain. Another characteristic feature of the NM-domain is the presence of the Q/N-rich region that is typical for many amyloidogenic proteins.[13, 14] Since the NM-domain of yeast Sup35p is responsible for protein aggregation and C-domain has non-prion functions, it is reasonable to hypothesize that NM-region and C-domain of Sup35p were divided at the DNA level at the certain time point of protein evolution.

Next, we used known information on the sequence homology between actin and Ssa1[57] to search for co-partners of Sup35p and EF1A. To orient ourselves among 104 potential co-partners of these two proteins, we used another established fact, namely that the heat shock proteins are accumulated at the *[PSI+]* fibril formation area.[24] Among those heat shock proteins, Ssa1 was reported as an interaction partner of elongation factor 1.[41] Therefore, based on this evidence we selected actin and Ssa1 as potential co-partners of two yeast proteins, Sup35pC, and EF1A. Due to the lack of data on exact localization of partner binding sites on Sup35p, we assumed that Sup35pC partners are included to the list of the Sup35p partners. Finally, among the 18 partners of human ERF3A, we selected PIK3R1 since this protein is involved in the indirect modulation of actin through the mTORc2 pathway.[43]

Analysis of the available structural information revealed that there are some structural homologies between partners (yeast actin, yeast Ssa1, and human PIK3R1). In fact, in agreement with earlier studies on sequence similarities, we found that yeast actin and Ssa1 do possess noticeable structural similarity (Figure 2). There are also several PIK3R1 regions with some structural homology to yeast actin, although the homology levels were noticeably lower than the structural homology of effectors, Sup35pC, yeast EF1A, and human ERF3A (Figure 1). More detailed analysis of the actin/Ssa1/PIK3R1 MoRF region which is present in all partners (residues 8-20, 7-19, and 654-673 in actin, Ssa1, and PIK3R1, respectively) revealed that this region possess common β-loop-β motif (Figure 4). Furthermore, Figure 5 shows that these segments have similar disorder patterns thereby providing further support to the hypothesis of

their functional similarity. Assuming that the interaction between effectors and their partners is modulated by intrinsic disorder and assuming that potential partner binding sites are similarly positioned within the structures of effectors and are evolutionary conserved, the most probable locations of the sites of effectors responsible for binding of partners are regions containing residues 85-91, 87-91, and 152-158 in Sup35pC, EF1A, and ERF3A, respectively (Table 9 and Figure 3).

Our analysis indicated that there are several ways of how effectors can interact with partners. This analysis was based on the earlier observed homology between actin and Ssa1[57] and showed that pair-wise interactions are possible between Sup35pC and Ssa1 (7-376), Sup35pC and actin (8-349), EF1A and actin (8-349), and ERF3A and PIK3R1 (Table 11, Supplementary Table 1). During this analysis, conserved binding region (MoRF) was detected through iLoops algorithm among effectors Sup35pC, EF1A, and ERF3A.This region is indicated by the red box in Figure 3A. However, only the actin MoRF, which is marked by red box in Figure 3B, was detected as a potential interaction site during the analysis among partners (Supplementary Table 1). One of possible reasons for this result is that partners did not possess a meaningful sequence similarity with PIK3R1. In fact, PIK3R1 possessed the lowest sequence similarity with other proteins studied here, whereas Ssa1and actin both have relatively high similarities (see Figures 2 and 3).[57] Nevertheless, a fragment of PIK3R1 has structural similarity with actin, as shown in Figure 4. Also, Ssa1 has noticeable structural similarity with actin.[57] Therefore, despite the lack of the obvious sequence homology, PIK3R1 and Ssa1 possess regions structurally similar were not detected. Although the analysis didn't show sequence, and structure based potential interaction sites on PIK3R1, and Ssa1, it still showed that actin's predicted region has potential interaction site (Supplementary Table 1).

Therefore, our analysis revealed that Sup35pC might be involved in interaction with actin, directly or indirectly. This conclusion is supported indirectly by the fact that all proteins analyzed in this work are hybrid proteins that possess both ordered and intrinsically disordered

regions. Intrinsically disordered proteins or protein regions are known to be characterized by the remarkable structural and functional plasticity.[67, 93, 94] One of the consequences of this plasticity is the ability of intrinsically disordered protein to be involved in moonlighting activities.[95] Curiously, it was already emphasized that one of the Sup35p homologues, eukaryotic polypeptide elongation factor EF-1, is a protein with moonlighting functions.[35] We assume that the intrinsically disordered nature of some of the Sup35pC regions can define the structural heterogeneity and functional promiscuity of this protein.

The major inference of our research is the important conclusion that yeast Sup35pC is not only an important part of yeast prion, but also can play a number of crucial roles at the prion-independent stages of the cell cycle. Of a particular interest in this respect is a potential role of Sup35pC in the cytoskeleton organization during mitosis. In fact, although Sup35p and another polypeptide chain release factor, Sup45p (also known as eRF1), are responsible for translation termination, they are not the only proteins involved in this process in yeast, and several other proteins were recently identified that were shown to be involved in interaction with yeast eRF1 and eRF3 and to be able to influence the efficiency of translation termination.[65] Among these important modulators of the eRF1/eRF3 activity are several proteins (such as Upf1p, Mtt1p, and Itt1p), which have significant nontranslational functions and link translation with other cellular processes.[96-98] Furthermore, it is not only the partners of eRF1 and eRF3, which might have nontranslational functions. In fact, it has been emphasized that similar to many other components of the translation apparatus, eRF3 by itself may function in processes other than translation. For example, the reduced expression of the *Drosophila melanogaster* eRF3 in the fly testes produced noticeable morphological changes, with clear cytoskeleton defects in spermatids and with abnormal meiotic chromosome segregation.[99] Also, mutations in the *S. cerevisiae SUP35* and *SUP45* genes were identified that lead to the increased sensitivity to the microtubule-poisoning drug benomyl and affected chromosome segregation at anaphase.[100] Finally, compelling direct evidence was found for the interrelation between translation and

cytoskeleton were obtained for the elongation factor eEF1A, which is similar to the C-domain of eRF3.[101] Here, eEF1A was shown to be the most abundant actin-binding protein in different eukaryotic organisms, being able to bind and bundle actin in *S. cerevisiae*[102] in a Bni1p-dependent manner,[103] and being able to sever microtubules.[104] Based on the sequence and structural similarities between the eEF1A and the C-domain of eRF3, one might expect that Sup35p can be involved in the cytoskeleton remodeling too. It is possible that effect on translation termination could account for changes in yeast morphology. However, based on our studies, we hypothesize that this option alone does not account for changes in cytoskeleton structure. Further research is needed for better understanding of the multitude of functional implications of this enigmatic protein.

References

1. P. Mugnier and M. F. Tuite, *Biochemistry. Biokhimiia*, 1999, 64, 1360-1366.
2. S. Inge-Vechtomov, G. Zhouravleva and M. Philippe, *Biology of the cell / under the auspices of the European Cell Biology Organization*, 2003, 95, 195-209.
3. I. Stansfield, K. M. Jones, V. V. Kushnirov, A. R. Dagkesamanskaya, A. I. Poznyakovski, S. V. Paushkin, C. R. Nierras, B. S. Cox, M. D. Ter-Avanesyan and M. F. Tuite, *The EMBO journal*, 1995, 14, 4365-4373.
4. E. Z. Alkalaeva, A. V. Pisarev, L. Y. Frolova, L. L. Kisselev and T. V. Pestova, *Cell*, 2006, 125, 1125-1136.
5. C. Fabret, B. Cosnier, S. Lekomtsev, S. Gillet, I. Hatin, P. Le Marechal and J. P. Rousset, *BMC molecular biology*, 2008, 9, 22.
6. B. S. Cox, M. F. Tuite and C. S. McLaughlin, *Yeast*, 1988, 4, 159-178.
7. M. D. Ter-Avanesyan, A. R. Dagkesamanskaya, V. V. Kushnirov and V. N. Smirnov, *Genetics*, 1994, 137, 671-676.
8. R. B. Wickner, *Science*, 1994, 264, 566-569.
9. S. V. Paushkin, V. V. Kushnirov, V. N. Smirnov and M. D. Ter-Avanesyan, *The EMBO journal*, 1996, 15, 3127-3134.
10. M. D. Ter-Avanesyan, V. V. Kushnirov, A. R. Dagkesamanskaya, S. A. Didichenko, Y. O. Chernoff, S. G. Inge-Vechtomov and V. N. Smirnov, *Mol Microbiol*, 1993, 7, 683-692.
11. S. M. Doel, S. J. McCready, C. R. Nierras and B. S. Cox, *Genetics*, 1994, 137, 659-670.
12. A. Baudin-Baillieu, C. Fabret and O. Namy, *Prion*, 2011, 5, 299-304.
13. E. D. Ross, A. Minton and R. B. Wickner, *Nature cell biology*, 2005, 7, 1039-1044.
14. S. G. Inge-Vechtomov, G. A. Zhouravleva and Y. O. Chernoff, *Prion*, 2007, 1, 228-235.
15. M. F. Perutz, B. J. Pope, D. Owen, E. E. Wanker and E. Scherzinger, *Proceedings of the National Academy of Sciences of the United States of America*, 2002, 99, 5596-5600.

16. A. Santoso, P. Chien, L. Z. Osherovich and J. S. Weissman, *Cell*, 2000, 100, 277-288.

17. C. W. Helsen and J. R. Glover, *The Journal of biological chemistry*, 2012, 287, 542-556.

18. J. A. Toombs, N. M. Liss, K. R. Cobble, Z. Ben-Musa and E. D. Ross, *PloS one*, 2011, 6, e21953.

19. V. V. Kushnirov, N. V. Kochneva-Pervukhova, M. B. Chechenova, N. S. Frolova and M. D. Ter-Avanesyan, *The EMBO journal*, 2000, 19, 324-331.

20. U. Baxa, P. W. Keller, N. Cheng, J. S. Wall and A. C. Steven, *Mol Microbiol*, 2011, 79, 523-532.

21. S. N. Parham, C. G. Resende and M. F. Tuite, *The EMBO journal*, 2001, 20, 2111-2119.

22. P. Satpute-Krishnan, S. X. Langseth and T. R. Serio, *PLoS biology*, 2007, 5, e24.

23. Y. N. Park, D. Morales, E. H. Rubinson, D. Masison, E. Eisenberg and L. E. Greene, *PloS one*, 2012, 7, e37692.

24. H. R. Saibil, A. Seybert, A. Habermann, J. Winkler, M. Eltsov, M. Perkovic, D. Castano-Diez, M. P. Scheffer, U. Haselmann, P. Chlanda, S. Lindquist, J. Tyedmers and A. S. Frangakis, *Proceedings of the National Academy of Sciences of the United States of America*, 2012, 109, 14906-14911.

25. F. Chiappori, I. Merelli, G. Colombo, L. Milanesi and G. Morra, *PLoS computational biology*, 2012, 8, e1002844.

26. L. Xu, N. Hasin, M. Shen, J. He, Y. Xue, X. Zhou, S. Perrett, Y. Song and G. W. Jones, *PLoS computational biology*, 2013, 9, e1002896.

27. P. Liang and T. H. MacRae, *Journal of cell science*, 1997, 110 (Pt 13), 1431-1440.

28. G. M. Altschuler and K. R. Willison, *Journal of the Royal Society, Interface / the Royal Society*, 2008, 5, 1391-1408.

29. M. A. Kabir, W. Uddin, A. Narayanan, P. K. Reddy, M. A. Jairajpuri, F. Sherman and Z. Ahmad, *Journal of amino acids*, 2011, 2011, 843206.

30. Y. Song, Y. X. Wu, G. Jung, Y. Tutar, E. Eisenberg, L. E. Greene and D. C. Masison, *Eukaryotic cell*, 2005, 4, 289-297.

31. A. S. Borchsenius, R. D. Wegrzyn, G. P. Newnam, S. G. Inge-Vechtomov and Y. O. Chernoff, *The EMBO journal*, 2001, 20, 6683-6691.

32. C. T. Simons, A. Staes, H. Rommelaere, C. Ampe, S. A. Lewis and N. J. Cowan, *The Journal of biological chemistry*, 2004, 279, 4196-4203.

33. I. E. Vainberg, S. A. Lewis, H. Rommelaere, C. Ampe, J. Vandekerckhove, H. L. Klein and N. J. Cowan, *Cell*, 1998, 93, 863-873.

34. K. I. Brackley and J. Grantham, *Experimental cell research*, 2010, 316, 543-553.

35. S. Ejiri, *Bioscience, biotechnology, and biochemistry*, 2002, 66, 1-21.

36. R. A. Gungabissoon, S. Khan, P. J. Hussey and S. K. Maciver, *Cell motility and the cytoskeleton*, 2001, 49, 104-111.

37. K. Morita, F. Bunai and O. Numata, *Zoological science*, 2008, 25, 22-29.

38. F. Bunai, K. Ando, H. Ueno and O. Numata, *Journal of biochemistry*, 2006, 140, 393-399.

39. A. Doyle, S. R. Crosby, D. R. Burton, F. Lilley and M. F. Murphy, *Journal of structural biology*, 2011, 176, 370-378.

40. W. Yang and W. F. Boss, *The Journal of biological chemistry*, 1994, 269, 3852-3857.

41. Y. Gong, Y. Kakihara, N. Krogan, J. Greenblatt, A. Emili, Z. Zhang and W. A. Houry, *Molecular systems biology*, 2009, 5, 275.

42. C. Kong, K. Ito, M. A. Walsh, M. Wada, Y. Liu, S. Kumar, D. Barford, Y. Nakamura and H. Song, *Molecular cell*, 2004, 14, 233-245.

43. H. Populo, J. M. Lopes and P. Soares, *International journal of molecular sciences*, 2012, 13, 1886-1918.

44. J. Wang, K. Huo, L. Ma, L. Tang, D. Li, X. Huang, Y. Yuan, C. Li, W. Wang, W. Guan, H. Chen, C. Jin, J. Wei, W. Zhang, Y. Yang, Q. Liu, Y. Zhou, C. Zhang, Z. Wu, W. Xu,

Y. Zhang, T. Liu, D. Yu, L. Chen, D. Zhu, X. Zhong, L. Kang, X. Gan, X. Yu, Q. Ma, J. Yan, L. Zhou, Z. Liu, Y. Zhu, T. Zhou, F. He and X. Yang, *Molecular systems biology*, 2011, 7, 536.

45. Y. R. Chin and A. Toker, *Molecular cell*, 2010, 38, 333-344.

46. V. Zinzalla, D. Stracka, W. Oppliger and M. N. Hall, *Cell*, 2011, 144, 757-768.

47. E. Jacinto, R. Loewith, A. Schmidt, S. Lin, M. A. Ruegg, A. Hall and M. N. Hall, *Nature cell biology*, 2004, 6, 1122-1128.

48. F. M. Disfani, W. L. Hsu, M. J. Mizianty, C. J. Oldfield, B. Xue, A. K. Dunker, V. N. Uversky and L. Kurgan, *Bioinformatics*, 2012, 28, i75-83.

49. F. Sievers, A. Wilm, D. Dineen, T. J. Gibson, K. Karplus, W. Li, R. Lopez, H. McWilliam, M. Remmert, J. Soding, J. D. Thompson and D. G. Higgins, *Molecular systems biology*, 2011, 7, 539.

50. F. Kiefer, K. Arnold, M. Kunzli, L. Bordoli and T. Schwede, *Nucleic acids research*, 2009, 37, D387-392.

51. J. Kopp and T. Schwede, *Nucleic acids research*, 2004, 32, D230-234.

52. G. R. Andersen, L. Pedersen, L. Valente, I. Chatterjee, T. G. Kinzy, M. Kjeldgaard and J. Nyborg, *Molecular cell*, 2000, 6, 1261-1266.

53. S. Vorobiev, B. Strokopytov, D. G. Drubin, C. Frieden, S. Ono, J. Condeelis, P. A. Rubenstein and S. C. Almo, *Proceedings of the National Academy of Sciences of the United States of America*, 2003, 100, 5760-5765.

54. J. Liang, J. K. Chen, S. T. Schreiber and J. Clardy, *Journal of molecular biology*, 1996, 257, 632-643.

55. A. Musacchio, L. C. Cantley and S. C. Harrison, *Proceedings of the National Academy of Sciences of the United States of America*, 1996, 93, 14373-14378.

56. G. Siegal, B. Davis, S. M. Kristensen, A. Sankar, J. Linacre, R. C. Stein, G. Panayotou, M. D. Waterfield and P. C. Driscoll, *Journal of molecular biology*, 1998, 276, 461-478.

57. J. H. Hurley, *Annual review of biophysics and biomolecular structure*, 1996, 25, 137-162.

58. B. Aranda, H. Blankenburg, S. Kerrien, F. S. Brinkman, A. Ceol, E. Chautard, J. M. Dana, J. De Las Rivas, M. Dumousseau, E. Galeota, A. Gaulton, J. Goll, R. E. Hancock, R. Isserlin, R. C. Jimenez, J. Kerssemakers, J. Khadake, D. J. Lynn, M. Michaut, G. O'Kelly, K. Ono, S. Orchard, C. Prieto, S. Razick, O. Rigina, L. Salwinski, M. Simonovic, S. Velankar, A. Winter, G. Wu, G. D. Bader, G. Cesareni, I. M. Donaldson, D. Eisenberg, G. J. Kleywegt, J. Overington, S. Ricard-Blum, M. Tyers, M. Albrecht and H. Hermjakob, *Nature methods*, 2011, 8, 528-529.

59. S. Henikoff and J. G. Henikoff, *Proceedings of the National Academy of Sciences of the United States of America*, 1992, 89, 10915-10919.

60. M. Punta, P. C. Coggill, R. Y. Eberhardt, J. Mistry, J. Tate, C. Boursnell, N. Pang, K. Forslund, G. Ceric, J. Clements, A. Heger, L. Holm, E. L. Sonnhammer, S. R. Eddy, A. Bateman and R. D. Finn, *Nucleic acids research*, 2012, 40, D290-301.

61. H. Dinkel, S. Michael, R. J. Weatheritt, N. E. Davey, K. Van Roey, B. Altenberg, G. Toedt, B. Uyar, M. Seiler, A. Budd, L. Jodicke, M. A. Dammert, C. Schroeter, M. Hammer, T. Schmidt, P. Jehl, C. McGuigan, M. Dymecka, C. Chica, K. Luck, A. Via, A. Chatr-Aryamontri, N. Haslam, G. Grebnev, R. J. Edwards, M. O. Steinmetz, H. Meiselbach, F. Diella and T. J. Gibson, *Nucleic acids research*, 2012, 40, D242-251.

62. B. Xue, R. L. Dunbrack, R. W. Williams, A. K. Dunker and V. N. Uversky, *Biochimica et biophysica acta*, 2010, 1804, 996-1010.

63. J. Planas-Iglesias, M. A. Marin-Lopez, J. Bonet, J. Garcia-Garcia and B. Oliva, *Bioinformatics*, 2013, DOI: 10.1093/bioinformatics/btt401.

64. Y. Inagaki, C. Blouin, E. Susko and A. J. Roger, *Nucleic acids research*, 2003, 31, 4227-4237.

65. I. A. Valouev, V. V. Kushnirov and M. D. Ter-Avanesyan, *Cell motility and the cytoskeleton*, 2002, 52, 161-173.

66. S. Jones, M. Stewart, A. Michie, M. B. Swindells, C. Orengo and J. M. Thornton, *Protein Sci*, 1998, 7, 233-242.

67. V. N. Uversky, *Biochimica et biophysica acta*, 2013, 1834, 932-951.

68. B. He, K. Wang, Y. Liu, B. Xue, V. N. Uversky and A. K. Dunker, *Cell Res*, 2009, 19, 929-949.

69. P. Romero, Z. Obradovic, X. Li, E. C. Garner, C. J. Brown and A. K. Dunker, *Proteins*, 2001, 42, 38-48.

70. K. Peng, P. Radivojac, S. Vucetic, A. K. Dunker and Z. Obradovic, *BMC Bioinformatics*, 2006, 7, 208.

71. C. J. Oldfield, Y. Cheng, M. S. Cortese, P. Romero, V. N. Uversky and A. K. Dunker, *Biochemistry*, 2005, 44, 12454-12470.

72. Y. Cheng, C. J. Oldfield, J. Meng, P. Romero, V. N. Uversky and A. K. Dunker, *Biochemistry*, 2007, 46, 13468-13477.

73. K. Peng, S. Vucetic, P. Radivojac, C. J. Brown, A. K. Dunker and Z. Obradovic, *Journal of bioinformatics and computational biology*, 2005, 3, 35-60.

74. A. K. Dunker, M. M. Babu, E. Barbar, M. Blackledge, S. E. Bondos, Z. Dosztányi, H. J. Dyson, J. Forman-Kay, M. Fuxreiter, J. Gsponer, K.-H. Han, D. T. Jones, S. Longhi, S. J. Metallo, K. Nishikawa, R. Nussinov, Z. Obradovic, R. Pappu, B. Rost, P. Selenko, V. Subramaniam, J. L. Sussman, P. Tompa and V. N. Uversky, *Intrinsically Disordered Proteins*, 2013, 1.

75. W. Kabsch, H. G. Mannherz, D. Suck, E. F. Pai and K. C. Holmes, *Nature*, 1990, 347, 37-44.

76. J. A. Zahm, S. B. Padrick, Z. Chen, C. W. Pak, A. A. Yunus, L. Henry, D. R. Tomchick and M. K. Rosen, *Cell*, 2013, 155, 423-434.

77. E. Irobi, A. H. Aguda, M. Larsson, C. Guerin, H. L. Yin, L. D. Burtnick, L. Blanchoin and R. C. Robinson, *EMBO J.*, 2004, 23, 3599-3608.

78. A. Bertazzon, G. H. Tian, A. Lamblin and T. Y. Tsong, *Biochemistry*, 1990, 29, 291-298.

79. C. C. Contaxis, C. C. Bigelow and C. G. Zarkadas, *Can. J. Biochem.*, 1977, 55, 325-331.

80. T. Le Bihan and C. Gicquaud, *Biochem. Biophys. Res. Commun.*, 1993, 194, 1065-1073.

81. S. S. Lehrer and G. Kerwar, *Biochemistry*, 1972, 11, 1211-1217.

82. K. K. Turoverov, A. G. Biktashev, S. Y. Khaitlina and I. M. Kuznetsova, *Biochemistry*, 1999, 38, 6261-6269.

83. L. V. Tatunashvili and P. L. Privalov, *Biofizika*, 1984, 29, 583-585.

84. J. J. West, B. Nagy and J. Gergely, *The Journal of biological chemistry*, 1967, 242, 1140-1145.

85. I. M. Kuznetsova, S. Khaitlina, S. N. Konditerov, A. M. Surin and K. K. Turoverov, *Biophys. Chem.*, 1988, 32, 73-78.

86. K. K. Turoverov, I. M. Kuznetsova, S. Y. Khaitlina and V. N. Uverskii, *Prot. Pept. Lett.*, 1999, 6, 73-78.

87. K. K. Turoverov, I. M. Kuznetsova and V. N. Uversky, *Prog. Biophys. Mol. Biol.*, 2010, 102, 73-84.

88. O. I. Povarova, V. N. Uversky, I. M. Kuznetsova and K. K. Turoverov, *Intrinsically Disordered Proteins*, 2014.

89. V. V. Kushnirov, M. D. Ter-Avanesyan, M. V. Telckov, A. P. Surguchov, V. N. Smirnov and S. G. Inge-Vechtomov, *Gene*, 1988, 66, 45-54.

90. P. G. Wilson and M. R. Culbertson, *Journal of molecular biology*, 1988, 199, 559-573.

91. M. Kabani, B. Cosnier, L. Bousset, J. P. Rousset, R. Melki and C. Fabret, *Mol Microbiol*, 2011, 81, 640-658.

92. M. Kabani and R. Melki, *Prion*, 2011, 5, 277-284.

93. V. N. Uversky, *Current pharmaceutical design*, 2013, 19, 4191-4213.

94. K. K. Turoverov, I. M. Kuznetsova and V. N. Uversky, *Progress in biophysics and molecular biology*, 2010, 102, 73-84.

95. P. Tompa, C. Szasz and L. Buday, *Trends Biochem Sci*, 2005, 30, 484-489.

96. Y. Weng, K. Czaplinski and S. W. Peltz, *Molecular and cellular biology*, 1996, 16, 5491-5506.

97. K. Czaplinski, N. Majlesi, T. Banerjee and S. W. Peltz, *RNA*, 2000, 6, 730-743.

98. V. N. Urakov, I. A. Valouev, E. I. Lewitin, S. V. Paushkin, V. S. Kosorukov, V. V. Kushnirov, V. N. Smirnov and M. D. Ter-Avanesyan, *BMC molecular biology*, 2001, 2, 9.

99. J. Basu, B. C. Williams, Z. Li, E. V. Williams and M. L. Goldberg, *Cell motility and the cytoskeleton*, 1998, 39, 286-302.

100. A. S. Borchsenius, A. A. Tchourikova and S. G. Inge-Vechtomov, *Curr Genet*, 2000, 37, 285-291.

101. J. Condeelis, *Trends Biochem Sci*, 1995, 20, 169-170.

102. R. Munshi, K. A. Kandl, A. Carr-Schmid, J. L. Whitacre, A. E. Adams and T. G. Kinzy, *Genetics*, 2001, 157, 1425-1436.

103. M. Umikawa, K. Tanaka, T. Kamei, K. Shimizu, H. Imamura, T. Sasaki and Y. Takai, *Oncogene*, 1998, 16, 2011-2016.

104. N. Shiina, Y. Gotoh, N. Kubomura, A. Iwamatsu and E. Nishida, *Science*, 1994, 266, 282-285.

Figure Legends

Figure 1. Evaluating conservation of Sup35pC

A. Results of sequence alignment of EF1A (P02994) and Sup35pC (254-685 region of P05453 which corresponds to the residues 1-432 of Sup35pC) of *S. cerevisiae* by CLUSTAL Omega, Version 1.2.0. This analysis revealed the 35.1% sequence similarity.

B. Whole protein structural alignment of EF1A (green, 1-458, PDB ID: 1F60) and Sup35pC (cyan, 254-685 of yeast eRF3; same as Sup35pC, model based on PDB ID: 1R5B) by 'align' function of PyMOL 1.3. RMSD value is 17.6Å.

C. Domain level structural alignment of EF1A (green) and Sup35pC (cyan) by 'align' function of PyMOL 1.3. Domains are fragmented according to the conserved pattern at Figure 1A and [42]. RMSD values for structurally aligned domains 1, 2 and 3 are 2.02 Å, 0.864 Å, and 0.997 Å, respectively.

Figure 2. Evaluating conservation of partners.

A. Structural alignment of actin (blue, 8-349, PDB ID: 1YAG) and Ssa1 (red, 7-376, model based on PDB ID: 3C7N) by 'cealign' function of PyMOL 1.3. RMSD value is 5.04 Å.

Structural alignment of actin (blue, 8-349, PDB ID: 1YAG) and each of four portions of the PIK3R1: **B**. (pink, 3-85, PDB ID: 1PHT); **C**. (orange, 115-309, PDB ID: 1PBW); **D**. (purple, 324-433, model based on PDB ID: 2IUG); **E**. (wheat, 614-724, PDB ID: 1BFI). The RMSD values are 6.49Å, 8.61 Å, 7.46 Å, and 7.12 Å, correspondingly. **F**. Structural alignment of actin (blue, 8-349, PDB ID: 1YAG) and the fourth fragment of PIK3R1 (olive, 431-600, model based on the PDB ID: 2VIY). The RMSD value is 5.42Å.

Figure 3. Depiction of the sequence conservation, conserved functional motifs, and MoRF-containing regions.

A. Multiple sequence alignment of effectors. One conserved region containing MoRF and functional motif (LIG_FHA_2) was found. This region is positioned within the residues 86-92 of EF1A, 153-159 of ERF3A, and 86-91 of Sup35pC. Motif probabilities are all 0.0083.

B. Multiple sequence alignment of partners. One conserved region containing MoRF and conserved functional motifs was found. In actin, this region contains a functional motif MOD_N-GLC_1 (residues 11-16, probability 0.0050). In Ssa1 and PIK3R1, this region contains the TRG_ENDOCYTIC_2 motif (residues 13-16 and 8-11 in Ssa1 and PIK3R1, respectively) with the probability of 0.0026.

Figure 4. Structural conservation of the actin MoRF-containing region. A. Actin (residues 8-349, PDB ID: 1YAG) is shown as blue ribbon. Its MoRF (residues 11-15, shown by red) possesses β-loop-β pattern. Acting is aligned with the structure of the PIK3R1 fragment (residues 614-724, wheat ribbon, PDB ID: 1BFI). Position of the PIK3R1 loop region 650-657 also containing β-loop-β pattern is shown by green. Structural alignments of the actin fragment (residues 7-98, blue ribbon) and PIK3R1 fragment (residues 3-85, pink ribbon) using 'Align' (**B**) and 'CEAlign' functions (**C**), respectively.

Figure 5. Analysis of intrinsic disorder propensity in actin (red), Ssa1 (black), and PIK3R1 (green).

A. Disorder propensity of actin evaluated by PONDR® VLXT (solid red line), PONDR® VL3 (dashed dark red line), and PONDR-FIT (pink line). Light pink shadow around the PONDR-FIT curve represents the error distribution.

B. Disorder propensity of Ssa1 evaluated by PONDR® VLXT (solid black line), PONDR® VL3 (dashed dark gray line), and PONDR-FIT (solid gray line). Light gray shadow around the PONDR-FIT curve represents the error distribution.

C. Disorder propensity of PIK3R1 evaluated by PONDR® VLXT (solid green line), PONDR® VL3 (dashed dark-dark green line), and PONDR-FIT (solid green line). Light green shadow around the PONDR-FIT curve represents the error distribution.

D. Overlapped PONDR® VLXT curves for actin (red), Ssa1 (black), and PIK3R1 (green) represented for the full-length proteins.

E. Overlapped PONDR® VLXT curves for actin (red), Ssa1 (black), and PIK3R1 (green) represented for the N-terminal 250 residues of proteins.

Figure 6. Analysis of intrinsic disorder propensity in Sup35p (black), EF1A (red), and ERF3A (green).

A. Disorder propensity of Sup35p evaluated by PONDR® VLXT (solid black line), PONDR® VL3 (dashed dark gray line), and PONDR-FIT (solid gray line). Light gray shadow around the PONDR-FIT curve represents the error distribution.

B. Disorder propensity of EF1A evaluated by PONDR® VLXT (solid red line), PONDR® VL3 (dashed dark red line), and PONDR-FIT (pink line). Light pink shadow around the PONDR-FIT curve represents the error distribution.

C. Disorder propensity of ERF3A evaluated by PONDR® VLXT (solid green line), PONDR® VL3 (dashed dark-dark green line), and PONDR-FIT (solid green line). Light green shadow around the PONDR-FIT curve represents the error distribution.

D. Overlapped PONDR® VLXT curves for the aligned Sup35p (black), EF1A (red), and ERF3A (green) represented for the full-length proteins. Positions of EF1A and ERF3A are aligned to coincide with the position of Sup35p.

Table 1. List of ten proteins selected for the sequence homology analysis

No.	Organism	Accession ID (BLAST)	UniProt ID	Length	Score (BLASP)	E-value (BLASP)
1	*S.cerevisiae*	NP_010457.3	P05453	685	905	0.0
2	*X.tropicalis*	NP_001015805.2	Q5FVC1	558	528	0.0
3	*H.sapiens*	NP_001123479.1	P15170	499	525	0.0
4	*G.gallus*	NP_001129149.1	UPI0000E80F80	618	525	0.0
5	*M.musculus*	NP_032205.2	UPI00001F819E	632	524	3E-180
6	*O.latipes*	XP_004080171.1	UPI0002A47A4C	588	521	9E-180
7	*D.rerio*	NP_942101.1	Q7T358	577	520	2E-179
8	*D.melanogaster*	NP_001260416.1	M9PD08	495	512	2E-177
9	*C.intestinalis*	XP_002129073.2	UPI000180C788	550	514	3E-177
10	*C.elegans*	NP_001256292.1	O45622	532	470	3E-160

Table 2. List of UniProt ID of effectors and partners analyzed in this study

Function	No.	Name	Organism	UniProt ID
Effector	1	Sup35pC	*S.cerevisiae*	P05453*
	2	EF1A		P02994
	3	ERF3A	*H.sapiens*	P15170
Partner	1	Ssa1	*S.cerevisiae*	P10591
	2	Actin		P60010
	3	PIK3R1	*H.sapiens*	P27986

*Position 254-685 was used for the Sup35pC analysis

Table 3. Results of the multiple sequence alignments for the full length Sup35p and Sup35pC (before and after modification of the alignment protocol)

	Identity	Number of Identical positions	Number of Similar positions
Before modification*	22.1%	160	149
After modification*	36.7%	159	148

* Modification: We obtained Sup35pC conserved pattern showing portion of each protein, through 'slicing' technique of Python 3.3, as described in Materials and Methods section.

Table 4. List of the co-partners of yeast proteins Sup35p and EF1A, and partners of human protein ERF3A

Organism	UniProt ID	Organism	UniProt ID	Organism	UniProt ID
S.cerevisiae	O13539	*S.cerevisiae*	P32588	*S.cerevisiae*	P53849
	O94742		P32589		P60010
	P00360		P32628		Q00539
	P00925		P32767		Q01477
	P02829		P32770		Q02336
	P02992		P33201		Q02793
	P02994		P33308		Q03330
	P04147		P33416		Q03735
	P05317		P33418		Q03957
	P05453		P34078		Q04087
	P05737		P34160		Q04175
	P06105		P35207		Q04373
	P06244		P35732		Q04493
	P07347		P36008		Q06525
	P0CG63		P38181		Q07457
	P10080		P38633		Q07623
	P10081		P38764		Q08231
	P10591		P38828		Q08972
	P10592		P38886		Q12315
	P11076		P38934		Q12476
	P11484		P38996		Q12517
	P12385		P39076		Q99260
	P12612		P39079	*H.sapiens*	P98170
	P14741		P39101		Q99683
	P15108		P39706		P54253
	P16140		P39935		O75815
	P16521		P39987		Q9Y478
	P17883		P40150		Q14164
	P23638		P40395		P30480
	P23796		P40457		O00422
	P24869		P40568		P23508
	P25294		P41940		Q9UBN6
	P25454		P42935		Q9Y4K3
	P25491		P43588		P60520
	P25644		P47006		P40337
	P30771		P47017		P62330
	P31539		P48510		Q92731
	P32324		P52553		P27986
	P32368		P53011		Q14457
	P32471		P53617		Q92900-2
	P32583		P53741	N/A	

Table 5. Rank of average scores of sequence similarity between the 104 yeast proteins and one certain partner of human protein ERF3A

RANK	Human protein UniProt ID	Score	RANK	Human protein UniProt ID	Score
1	Q99683	1593	10	Q92731	989
2	Q92900-2	1460	11	Q14457	934
3	O75815	1265	12	Q9UBN6	822
4	P23508	1232	13	P30480	804
5	P54253	1203	14	Q9Y478	706
6	**P27986**	**1186**	15	P40337	612
7	Q14164	1166	16	P62330	547
8	P98170	1003	17	O00422	498
9	Q9Y4K3	997	18	P60520	415

Table 6. Rank of the sequence similarity scores of the 104 yeast proteins in relation to human protein PIK3R1

Rank	Yeast protein UniProt ID	Human protein UniProt ID	Score	Rank	Yeast protein UniProt ID	Human protein UniProt ID	Score
1	P40457	P27986	2143	53	Q03330	P27986	1151
2	P38181		2049	54	P34078		1146
3	P17883		1995	55	P38934		1145
4	P35207		1953	56	Q02336		1124
5	P06105		1882	57	P12385		1116
6	Q08972		1843	58	P00925		1104
7	Q03735		1800	59	P02994		1096
8	P32767		1764	60	P39706		1096
9	P40395		1732	61	P10081		1078
10	P33418		1724	62	P02992		1071
11	P30771		1723	63	P39101		1070
12	P16521		1710	64	P06244		1063
13	P38764		1682	65	P36008		1060
14	Q04175		1635	66	P32588		1054
15	P34160		1622	67	P25454		1050
16	P39935		1613	68	P32628		1047
17	Q01477		1595	69	P25491		1023
18	P31539		1591	**70**	**P60010**		**1021**
19	P32324		1563	71	Q02793		1019
20	P25644		1531	72	P41940		1018
21	P33416		1526	73	P0CG63		1016
22	P42935		1525	74	P53011		991
23	P02829		1446	75	Q04087		977
24	Q07457		1446	76	Q12476		975
25	P15108		1444	77	P48510		945
26	P32589		1426	78	P00360		931
27	P05453		1397	79	P25294		928
28	P38996		1393	80	P43588		923
29	Q04373		1385	81	P10080		870
30	P32770		1356	82	P14741		865
31	P32368		1343	83	P32583		864
32	P10592		1341	84	P05317		855
33	P39987		1341	85	O13539		838
34	**P10591**		**1340**	86	P23638		825
35	P40150		1299	87	P38886		798
36	P11484		1298	88	P07347		797
37	P35732		1272	89	P05737		791
38	P53617		1271	90	P47006		787

39	P40568		1268	91	Q12517		777
40	P04147		1251	92	P33201		775
41	P16140		1237	93	Q07623		745
42	P39079		1235	94	Q99260		719
43	P39076		1229	95	P32471		691
44	P23796		1226	96	P47017		665
45	P12612		1225	97	P11076		662
46	Q03957		1210	98	P38828		656
47	Q12315		1207	99	Q04493		606
48	P53741		1195	100	P33308		578
49	Q00539		1187	101	P53849		576
50	Q08231		1181	102	P38633		511
51	P24869		1180	103	P52553		483
52	Q06525		1173	104	O94742		400

Table 7. Results of the sequence alignments between one human partner and each one of the two yeast co-partners

Pair	Total Length	Identity	Number of Identical positions	Number of Similar positions
PIK3R1 *vs*. actin (P27985:P60010)	PIK3R1 : 724 Actin : 375	8.65%	66	119
PIK3R1 *vs*. Ssa1 (P27985:P10591)	PIK3R1 : 724 Ssa1 : 642	13.2%	109	200

Table 8. Results of the Pfam analysis of proteins analyzed in this study

Function	Protein	Pfam ID	Superfamily	Analyzed sequence	E-value
Effector	Sup35pC	GTP_EFTU	P-loop containing nucleoside triphospate hydrolase	5-225	2E-46
		GTP_EFTU_D2		249-317	3E-07
		GTP_EFTU_D3	N/A	322-430	1E-25
	EF1A	GTP_EFTU	P-loop containing nucleoside triphospate hydrolase	5-232	3E-57
		GTP_EFTU_D2		258-324	6E-17
		GTP_EFTU_D3	N/A	331-439	1E-34
	ERF3A	GTP_EFTU	P-loop containing nucleoside triphospate hydrolase	72-271	1E-48
		GTP_EFTU_D2		314-381	6E-07
		GTP_EFTU_D3	N/A	391-494	3E-22
Partner	actin	Actin	Actin-like ATPase	4-375	3E-161
	Ssa1	HSP70	Actin-like ATPase	1-602	5E-274
	PIK3R1	SH3_2	Src homology-3 domain	8-75	1E-04
		RhoGAP	GTPase activation domain	129-277	3E-31
		SH2	SH2, phosphotyrosine-recognition domain	333-408	9E-18
				624-698	3E-20

Table 9. Results of the MoRFpred analysis of proteins analyzed in this study

Function	Protein	MoRFs
Effector	Sup35pC	10-13 / 57-61 / 85-91 / 387-388 / 426-430
	EF1A	9-14 / 57-60 / 87-91 / 344 / 397
	ERF3A	21-27 / 45-52 / 74-79 / 80-83 / 121-128 / 152-158 / 429 /452 / 491-494
Partner	actin	11-15 / 90 / 372-375
	Ssa1	11-14 / 41-43 / 236 / 345-346 / 453-457 / 501-506 / 539-548 /570-577 / 600 / 634-641
	PIK3R1	8-13 / 55 / 69-78 / 109-119 / 242-243 / 268-269 / 292 / 329-334 / 450 /490 / 507-508 / 540-541 / 622 / 716-722

Table 10. Sequence alignments and MoRFpred-based ELM analysis

Function	Protein	Conserved Amino acids & MoRF containing motifs	MoRF containing common motifs	Common motifs	Total motifs
Effector	Sup35pC	1*	3*	26	104
	EF1A				87
	ERF3A				115
Partner	actin	1*	3*	28	104
	Ssa1				158
	PIK3R1				221

* Motif names are given in Figure 3.

Table 11. Result of the iLoops-based prediction of protein-protein interaction

Pair	Prediction	Score	Inferred precision	No. of Positive signals	No. of Negative signals
Sup35pC *vs.* actin_8-349	Yes	0.767	0.86±0.01	9546	267
Sup35pC *vs.* Ssa1_7-376	Yes	0.591	0.65±0.02	610	649
EF1A *vs.* actin_8-349	Yes	0.779	0.86±0.01	12890	653
ERF3A *vs.* PIK3R1	Yes	0.878	0.91±0.023	688	40

A

```
P02994|EF1A_YEAST MGKEKSHINVVVIGHVDSGKSTTTGHLIYKCGGIDKRTIEKFEKEAAELGKGSFKYAWVL 60
eRF3C             MFGGKDHVSLIFMGHVDAGKSTMGGNLLYLTGSVDKRTIEKYEREAKDAGRQGWYLSWVM 60
                  *   *.*:.::.:****:****  *.*:*  *.:********:*:** : *: .:  :**:

P02994|EF1A_YEAST DKLKAERERGITIDIALWKFETPKYQVTVIDAPGHRDFIKNMITGTSQADCAILIIAGGV 120
eRF3C             DTNKEERNDGKTIEVGKAYFETEKRRYTILDAPGHKMYVSEMIGGASQADVGVLVISARK 120
                  *. * **: * **::.   *** * : *::*****: ::.:** *:**** .:*:*:.

P02994|EF1A_YEAST GEFEAGISKDGQTREHALLAFTLGVRQLIVAVNKMD--SVKWDESRFQEIVKETSNFIKK 178
eRF3C             GEYETGFERGGQTREHALLAKTQGVNKMVVVVNKMDDPTVNWSKERYDQCVSNVSNFLRA 180
                  **:*:*:.: ********** * **.:::*.*****  :*:*.:.*::: *.:.***::

P02994|EF1A_YEAST VGYNPKT-VPFVPISGWNGDNMIEA--TTNAPWYKGWEKETKAGVVKGKTLLEAIDAIEQ 235
eRF3C             IGYNIKTDVVFMPVSGYSGANLKDHVDPKECPWYTG----------PTLLEYLDTMNH 228
                  :*** ** * *:*:**:.* *: :    .:.***.*            **** :*::::

P02994|EF1A_YEAST PSRPTDKPLRLPLQDVYKIGGIGTVPVGRVETGVIKPGMVVTFAPAGVTTEVKSVEMH-H 294
eRF3C             VDRHINAPFMLPIAA--KMKDLGTIVEGKIESGHIKKGQSTLLMPNKTAVEIQNIYNETE 286
                   .*  : *: **:    *:  :**:  *::*:* ** *  . : *  .:.*::.:  . .

P02994|EF1A_YEAST EQLEQGVPGDNVGFNVKNVSVKEIRRGNVCGDAKNDPPKGCASFNATVIVLNHPGQISAG 354
eRF3C             NEVDMAMCGEQVKLRIKGVEEEDISPGFVLTS-PKNPIKSVTKFVAQIAIVELKSIIAAG 345
                  :::: .: *::* :.:* *. ::*  * *  .  ::* *. :.* * : :::  . *:**

P02994|EF1A_YEAST YSPVLDCHTAHIACRFDELLEKNDRRSGKKLEDHPKFLKSGDAALVKFVPSKPMCVEAFS 414
eRF3C             FSCVMHVHTAIEEVHIVKLLHKLEKGTNRKSKKPPAFAKKGMKVIAVLETEAPVCVETYQ 405
                  :* *:. ***    :: :**.* :: : :* :. * * *.*  .:. :  . *:***::.

P02994|EF1A_YEAST EYPPLGRFAVRDMRQTVAVGVIKSVDKTEKAAKVTKAAQKAAKK 458
eRF3C             DYPQLGRFTLRDQGTTIAIGKIVKIAE----------------- 432
                  :** ****::**   *:*:* * .: :
```

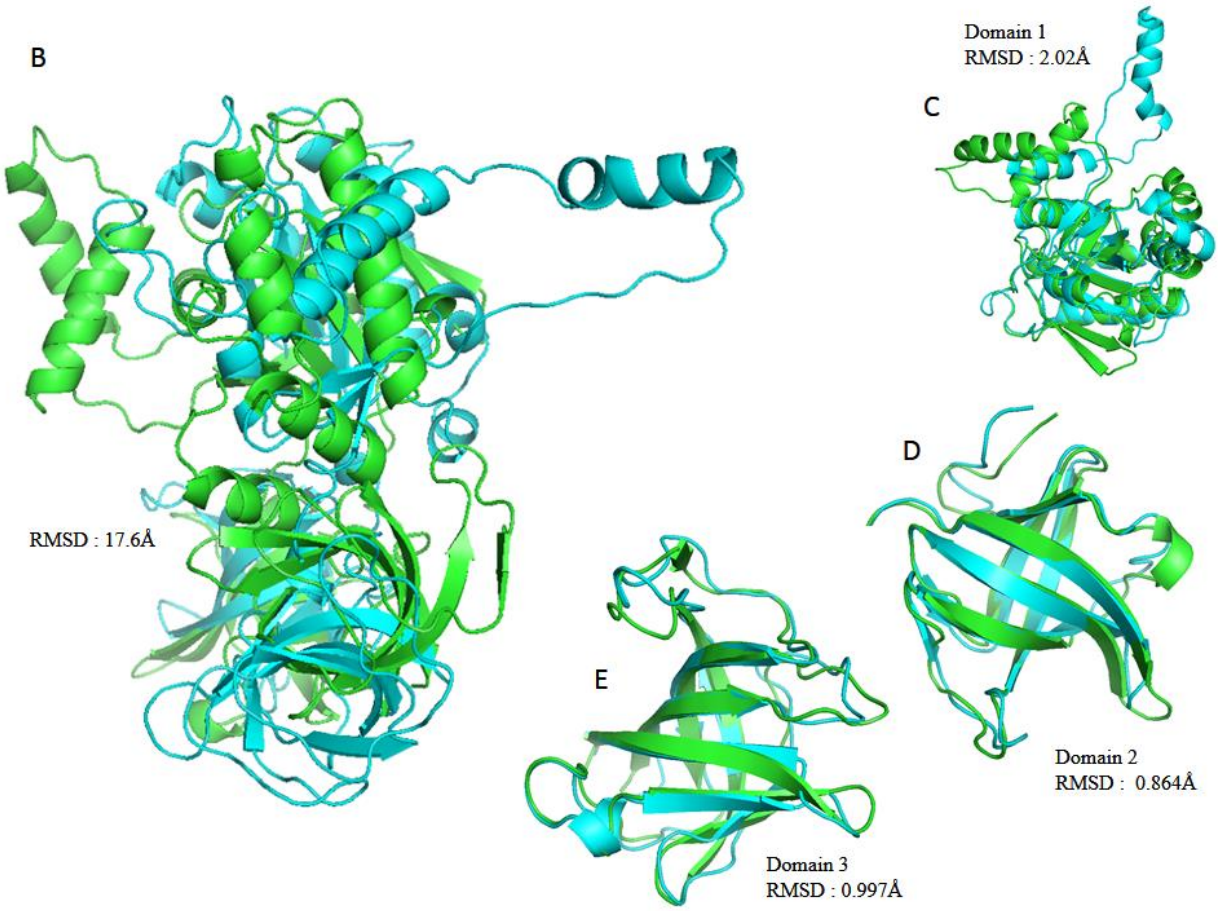

Figure 1

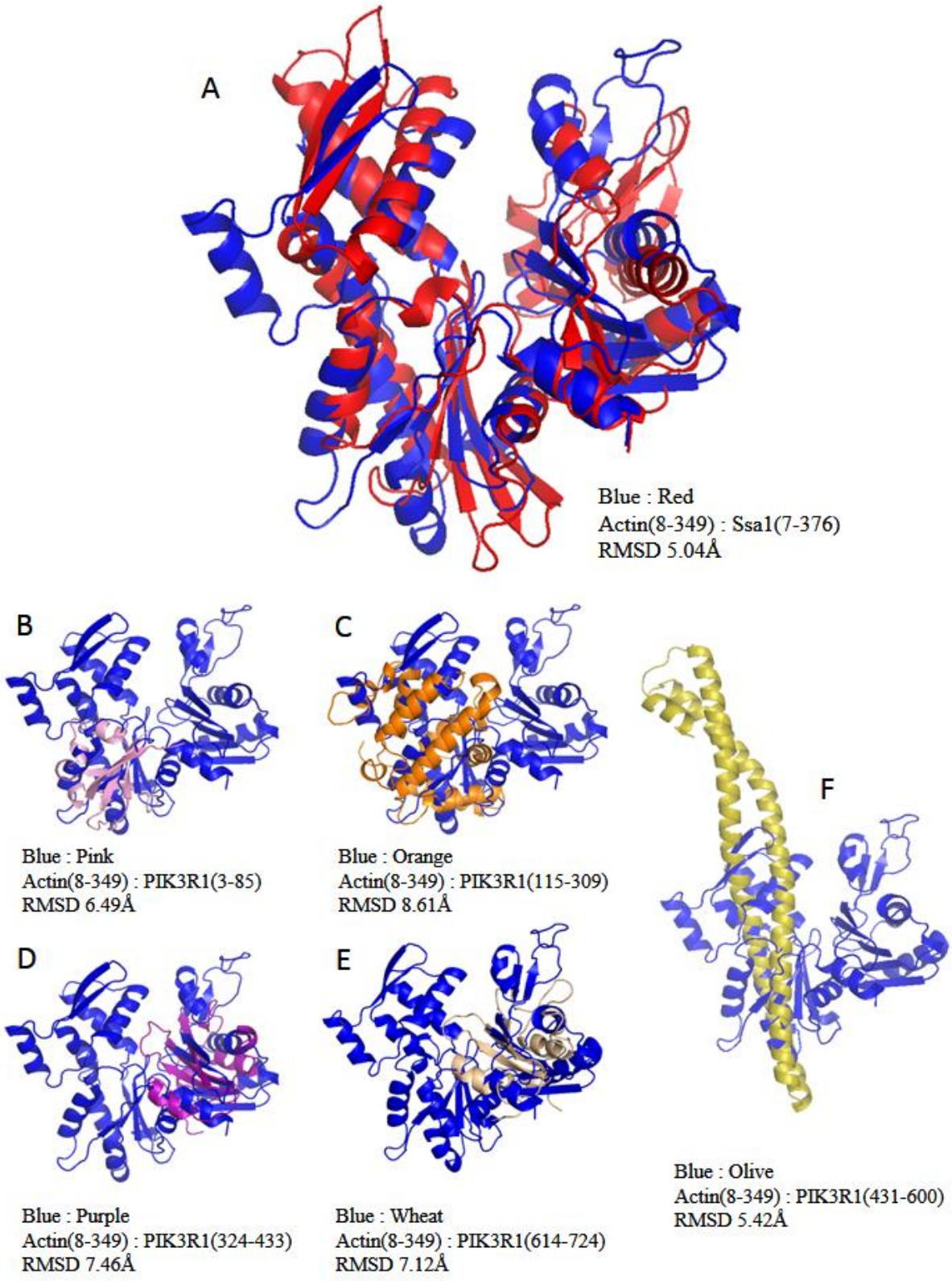

Figure 2

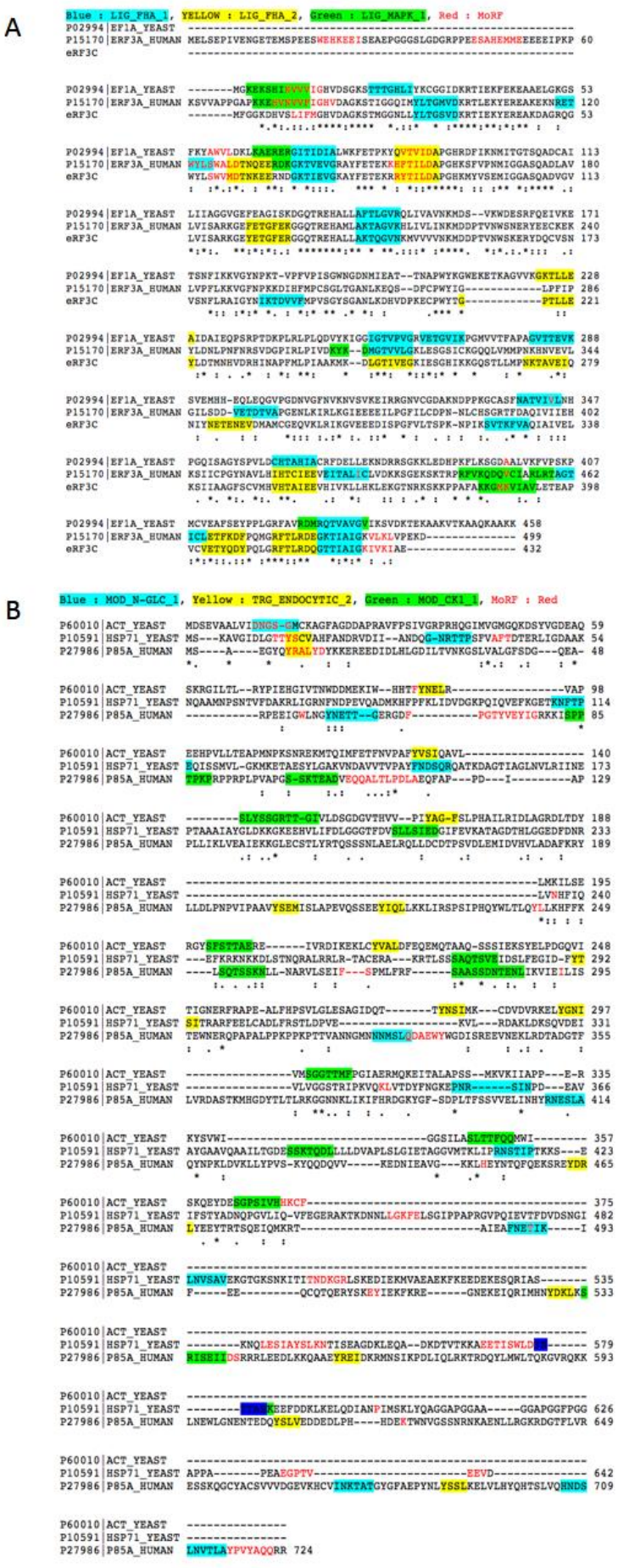

Figure 3

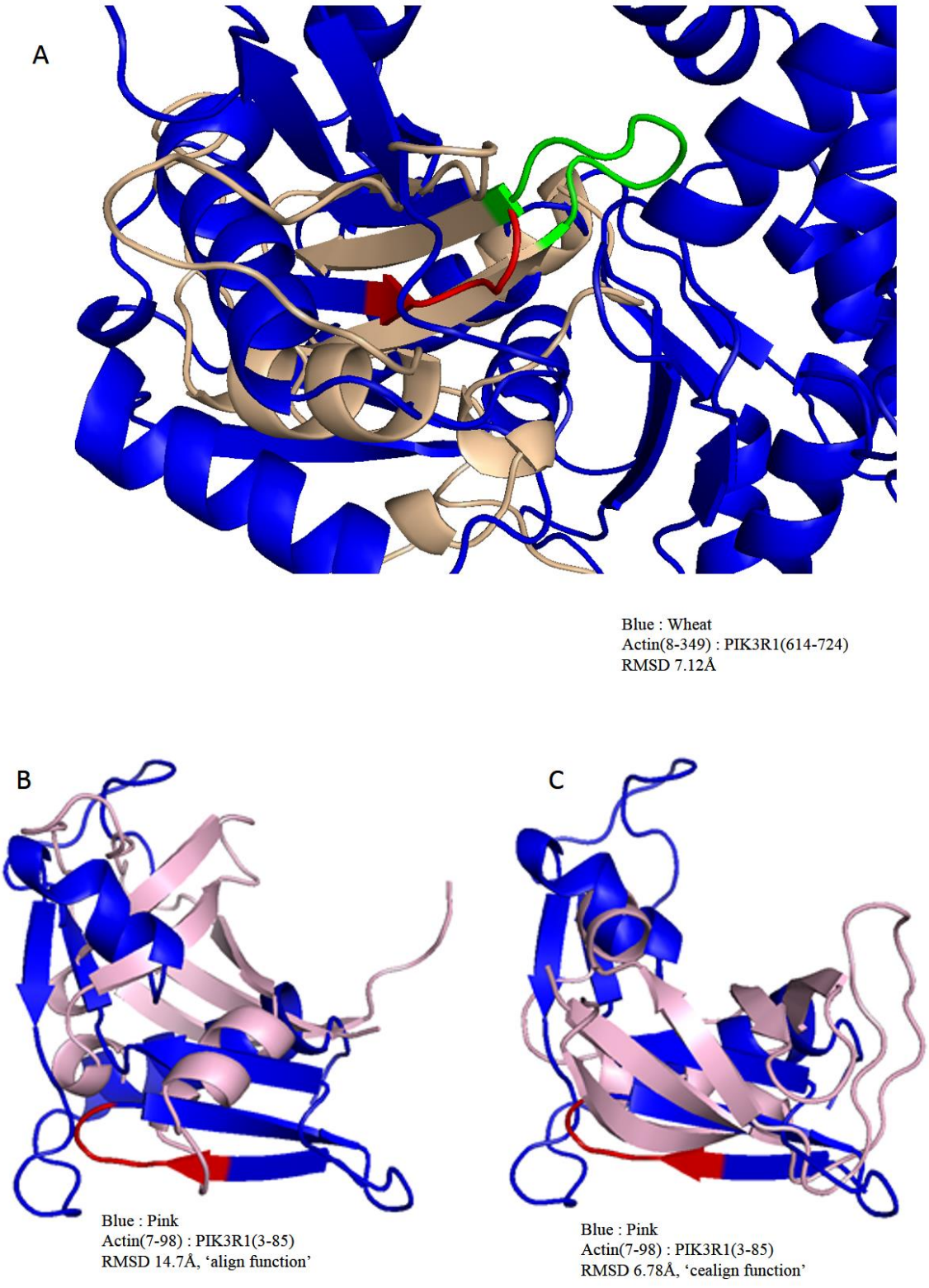

Figure 4

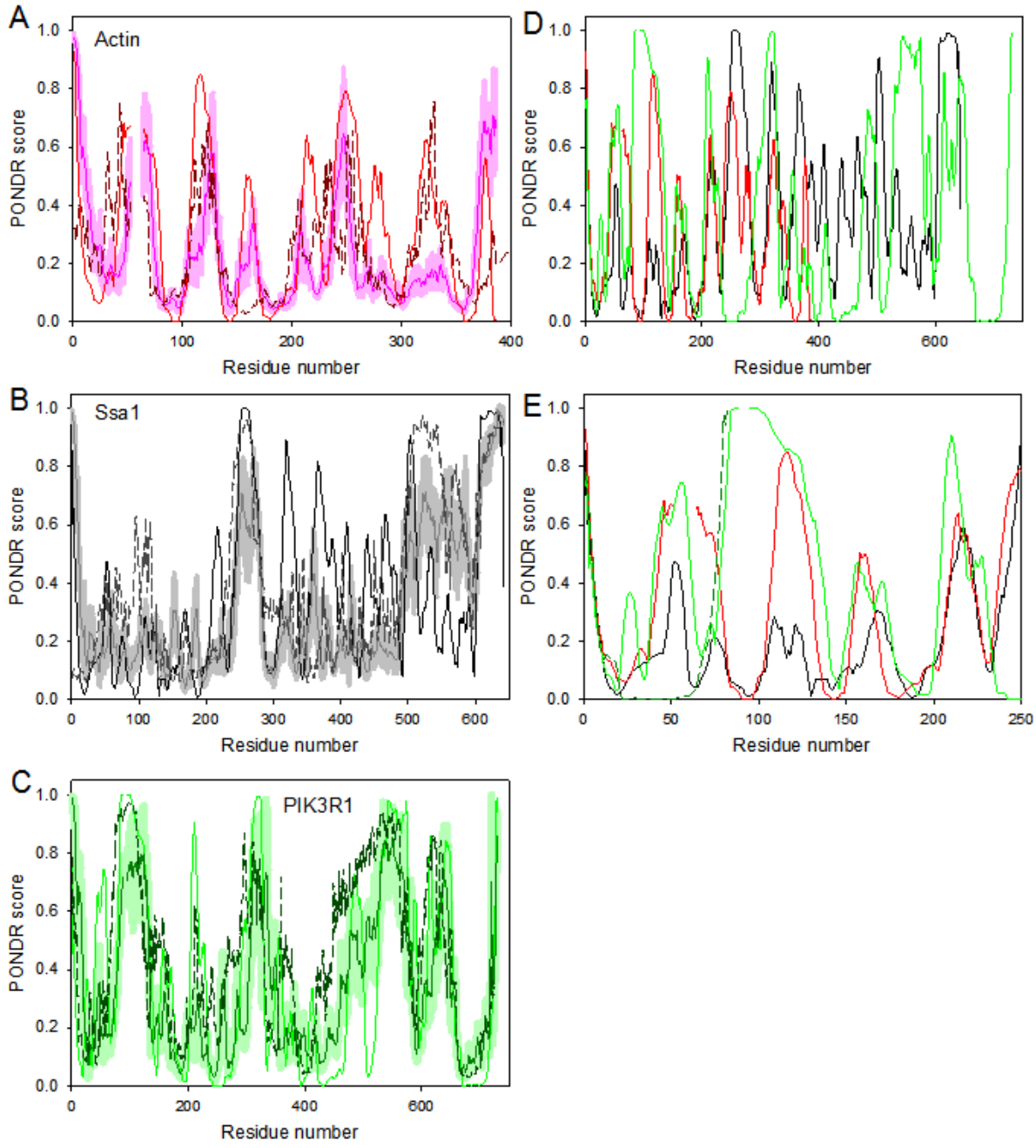

Figure 5

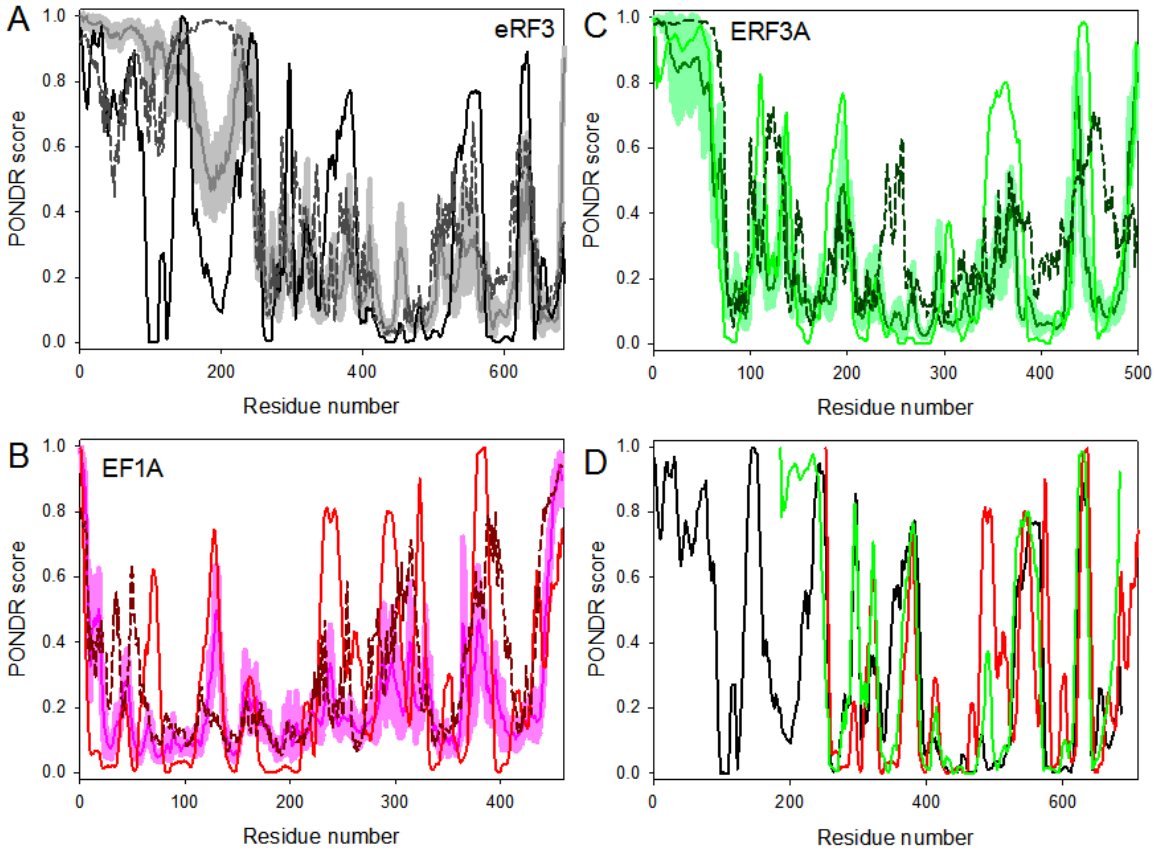

Figure 6